Effects of Al concentration on photovoltaic property of ZnO:Al/*p*-type Si by pulsed filtered cathodic vacuum arc deposition system

D. K. TAKCI[a], E. SENADIM TUZEMEN[b,*], S. YILMAZ[a], R. ESEN[a]
[a]*Department of Physics, Cukurova University, 01330 Adana, Turkey*
[b]*Nanophotonics Center, Department of Physics, Cumhuriyet University, 58140 Sivas, Turkey*

The effects of Al concentration on XPS, Raman, Hall and photovoltaic properties of Al-doped ZnO films were investigated onto Si (100) substrate by pulsed filtered cathodic vacuum arc deposition (PFCVAD) system, at room temperature. The Al doping effects in ZnO was performed by Raman measurements. The chemical state of ZnO:Al (AZO) films on Si substrate was investigated by using X-ray photoelectron spectroscopy (XPS). Hall Effect measurements were applied to characterize the electrical properties. Effect of doping concentration on photovoltaic property was also studied.

(Receievd October 19, 2014; accepted October 28, 2015)

Keywords: Al doped ZnO, Photovoltaic property, Pulsed filtered cathodic vacuum arc deposition

1. Introduction

ZnO thin films have attracted a great attention due to an exciton binding energy up to 60 meV, a wide and direct-bandgap semiconductor with an energy gap of 3.37 eV at 300 K [1], They are one of the promising candidate for fabricating surface acoustic wave instruments, gas sensors, solar cells and heat reflecting windows [2-4]. The most matured semiconductor technology is undoubtedly the Si technology. The advantages of this technology are that Si is an inexpensive and abundant element. This technology that enable ZnO thin film growths on Si due to these properties of its, is an important area of several applications such as n-ZnO/p-Si heterojunction photodiodes [4-6]. Zinc oxide is not an efficient donors because of its native point defects, but it is a highly resistive in the undoped state.When ZnO thin films were doped with IIIrd group elements such as B, Al, Ga, In, Ti, films with high quality, conductivity and transmittance in the visible region were obtained [7]. Because of relatively durable, soft, white, ductile, lightweight and malleable metal depending on the surface roughness, aluminum has the most promising element. Transparent conductive oxides (TCO) doped by metal oxides, are used in optoelectronic devices. TCO thin films have been generally used as transparent conductive electrodes in photovoltaic applications and display devices [8-12]. Aluminum-doped zinc-oxide (AZO), indium-doped cadmium-oxide [13] and tin-doped indium-oxide [14] have been proposed as alternative materials for transparent conductive oxides (TCO). Among TCO films, Al doped ZnO (AZO) films are being considered as manufacturing transparent electrodes due to their important properties such as an inexpensive, a nontoxic nature, a good electrical conductivity, a good adhesion to substrate, a chemical inertness, a high luminous transmittance and a long term environmental stability [15-18].

For the Al doped ZnO films preparation, different techniques have been used including sol–gel spin coating method [19], filtered cathodic vacuum arc technique [20], atomic layer deposition (ALD) [21], magnetron sputtering system [22], spray pyrolysis method [23], sol–gel multilayer dip-coating [24], direct-current (DC) magnetron sputtering [25], spin coating technique [26], the sol–gel technique [27], sol gel method using spin coating technique [28], direct current reactive sputtering [29] and pulsed laser deposition [30].

The electrical properties of Al doped zinc oxide thin films have been studied by many researchers. Tseng et al. showed an aqueous solution deposition technique to fabricate N-type ZnO and Al-doped ZnO (AZO) films at a very low temperature. They were used ZnO, Zn, and Al. Furthermore, the processing temperature was about 80 °C. The experimental results demonstrated that the resistivity of pristine ZnO and AZO films without any post-growth thermal annealing could be as low as ~2.0×10^{-2} Ω cm and ~8.4×10^{-3} Ω cm, respectively [31]. Lee et al. reported that highly conductive and transparent aluminum-doped zinc oxide (ZnO:Al) thin films were prepared using the filtered cathodic vacuum arc technique at relatively low temperatures. The ZnO:Al film properties were investigated under the influence of substrate temperature. They revealed that the optical, electrical and structural properties of the films depended directly on substrate temperature during deposition. The ZnO:Al films were prepared by using Zn–Al alloy targets with various Al content. The carrier concentration was determined to increase with increasing Al content, leading to reduction in

the resistivity. Although the mobility decreased slightly with increasing Al content, it was detected that the decrease was not sufficient to affect the trendof reduction in resistivity with increasing Al content. The lowest resistivity of 8×10^{-4} Ω cm was obtained for the Al-doped (5 at%) film prepared at a substrate temperature of 150 °C [20]. Vishwas et al. reported that ZnO:Al thin films were prepared on glass and silicon substrates by the sol–gel spin coating method. They fabricated the metal oxide semiconductor (MOS) capacitors using ZnO films deposited on silicon (100) substrates and studied electrical properties such as current versus voltage (I–V) and capacitance versus voltage (C–V) characteristics. They showed that the electrical resistivity decreased and the leakage current increased with an increase of annealing temperature [19]. Ahn et al. investigated the deposited AlZnO thin films with various Al/Zn composition ratios by atomic layer deposition (ALD) at 200 °C. The AlZnO films with an Al content of up to 10 at.% showed high conductivity while the increasing in the Al content resulted in the abrupt formation of an insulating oxide film. The lowest electrical resistivity of the ALD-deposited AlZnO film was 6.5×10^{-4} [Ω cm] at 5 at.% Al [21]. Gontijo et al. showed that thin n-type ZnO films doped with different atomic concentrations of aluminium were grown by filtered vacuum arc deposition (FVAD) on glass substrates. They investigated the effect of Al doping on ZnO films. They found the best values for an ideal aluminium percentage between 4 and 6 at.% [32]. Lei et al. investigated that the quality of AZO films grown on polyestersulfone (PES) depends on the deposition temperature and Al content. The optimal deposition temperature and Al content for AZO film were found as 185 C and 2.88 at%, respectively. Further, they reported that the increasing or decreasing in the deposition temperature and Al content degraded the quality of AZO films. They used as the anode for flexible OLED to the deposited optimal AZO film on the PES substrate. With OLEDs that commercial indium–tin-oxide (ITO) as the anode are used on glass, the similar performance was determined and enhanced characteristics to that of the commercial ITO anode on a flexible polyethylene naphthalate (PEN) substrate [33]. Zhang et al. showed that N-ZnO:Al (ZAO)/P-Si heterojunctions were prepared by direct current reactive sputtering. They examined by XRD, Hall effect measurement, open circuit voltage and short circuit current to determine the crystal structure, electrical property and photovoltaic effect. They showed that all the samples had a strong preferred *c*-axis orientation, and the crystal quality was destroyed with the increasing of Al concentration. The Hall effect measurement was showed that the carrier concentration increased with the addition of Al dopant. In order to investigation the influence mechanism of Al contents, they analyzed to the response spectra of these samples [29].

In our paper, we performed the deposition of undoped ZnO and ZnO:Al thin films by pulsed filtered cathodic vacuum arc deposition (PFCVAD) technique at room temperature, their raman, XPS and electrical properties.

2. Experimental details

The doped and undoped ZnO thin films were grown on Si (100) substrates by pulsed filtered cathodic vacuum arc deposition. In our previous studies, [7] we examined the effect of varying Al content by using metallic targets with Al content of 0, 2, 4, 6 and 10 %. During the growths, the substrate temperature was kept at room temperature, the base pressure of the deposition chamber was kept around 10^{-5} Torr and the working pressure was about 7×10^{-2} Torr. The base pressure and working pressure were controlled by Stanford Research Systems 4 Model PPM 100. High purity (99.999 % pure) oxygen gas was introduced into the chamber and controlled by multi gas controller. During the deposition process, trigger voltage and arc voltage were set to be 20 kV and 600 V, respectively.

Raman measurements were analyzed by Bruker Senterra Dispersive Raman Microscope that the 532 nm laser as an excitation source was used. The electrical properties of the films were determined by HMS-3000 system with the four-probe Van der Pauw technique. The chemical state of films were determined by PHI 5000 VERSAPROBE. The open-circuit voltages and the short circuit currents of AZO/p-Si heterojunctions with the different Al concentration were observed.

3. Result and discussion

3.1 Raman results of films

In our previous study, Raman scattering measurements were made to determine the structure and defect of undoped-ZnO lattice and the effect of Al incorporation in ZnO:Al thin films [7]. Fig. 1 shows the Raman scattering (RS) spectra of films, excited by the 532 nm laser lines using laser power of 5 mW. In undoped ZnO and Al-doped ZnO thin films were observed a raman peaks at about 439 cm^{-1}. This E_2(high) mode which is the characteristic for wurtzite hexagonal phase ZnO, is a Raman active optical phonon mode [34-36]. The increasing of the Al-doping concentration in ZnO films, is caused that Al ions are substituted for Zn ions in the ZnO lattice. This situation leads to decline in intensity of E_2 (high) peak and widen in the FWHM of its [35].

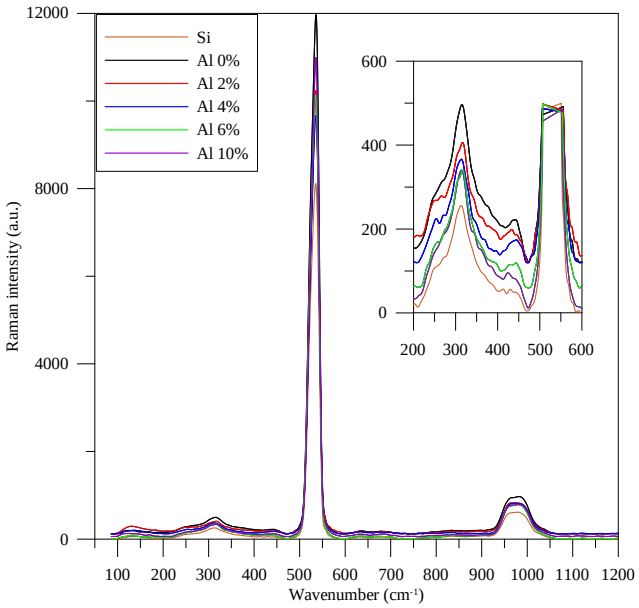

Fig. 1. The Raman spectra of Si, undoped ZnO and Al doped ZnO films (inset:200-600 cm^{-1})

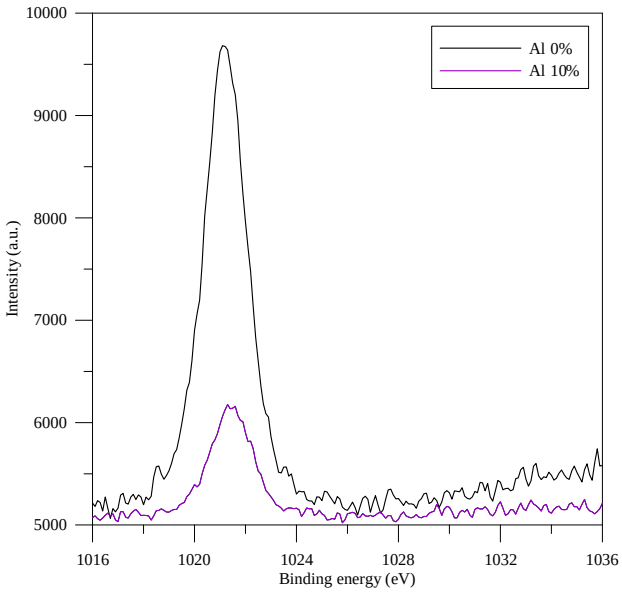

Fig. 2. Zn2p photoelectron peaks in the XPS spectrum of the undoped ZnO film and the 10% Al doped film

3.2 XPS results of undoped and Al-doped ZnO films on Si substrate

In this study, the chemical state of undoped ZnO and ZnO:Al (AZO) films were investigated by XPS. The presence of Al in the films was confirmed from the XPS result. With the XPS analysis, we measured the Zn2p, Ols and Al2p core level spectra.

The photoelectron peaks in the XPS spectra of Zn2p, Ols and Al2p were obtained for the undoped ZnO and Al-doped ZnO (AZO) thin films by different Al concentrations. The binding energies for all spectra were calibrated by taking the C1s peak, as the reference. As a result, Zn2p and Ols peaks were observed in undoped ZnO and doped ZnO films with 2%, 4% and 6% concentration of Al but Al2p peaks were not encountered. Al2p peak was only seen in the doped ZnO film with 10% Al.

For the undoped film, prominent peaks belonging to Zn and O were clearly seen in graphs. In this study, the binding energy of the area $Zn2p_{3/2}$ of this film was found as 1021.8±0.2 eV at peak position. This value was bigger than the value of ZnO in bulk structure. This shift in peak was originated from the zinc in the Zn-O bond charged positively and it was determined that Zn turn into Zn^{2+} form (Fig. 2) [37]. It was determined that the binding energy of Zn $2p_{3/2}$ in 10% Al doped films was as 1021.6 eV (Fig. 2).

In Fig. 3, we describe the O1s photoelectron spectra for undoped ZnO on Si substrate. The peak at the binding energies of 531.8 eV were detected in the O1s region. It is usually attributed to chemisorbed or dissociated oxygen or OH species on the surface of the ZnO thin film, such as adsorbed H_2O or adsorbed O_2 [38-40]. It was determined that the binding energy of O1s in 10% Al doped films was as 531.3 eV (Fig. 2).

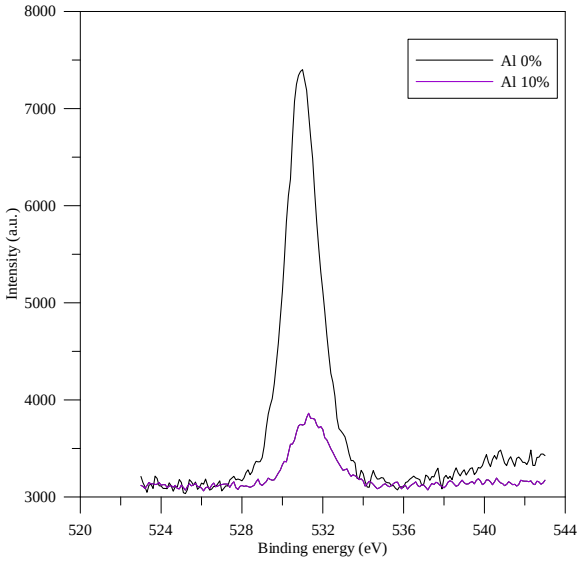

Fig. 3. O1s photoelectron peaks in the XPS spectrum of the undoped ZnO film and the 10% Al doped film

In Fig. 4, we described the Al2p photoelectron spectra for undoped ZnO on Si substrate. But, in the Al2p photoelectron spectra was not observed any peak.

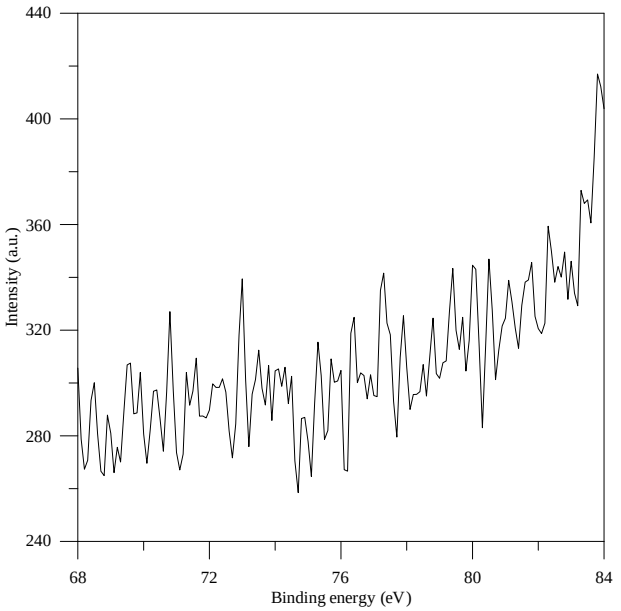

Fig. 4. Al2p photoelectron peak in the XPS spectrum of the undoped ZnO film

The binding energy of Al2p component at 74.1 eV may be due to the peak position of stoichiometric Al_2O_3 (Fig. 5) [38-42]. The 72.7±0.06 peak value belonging to metallic Al, was not observed [37].

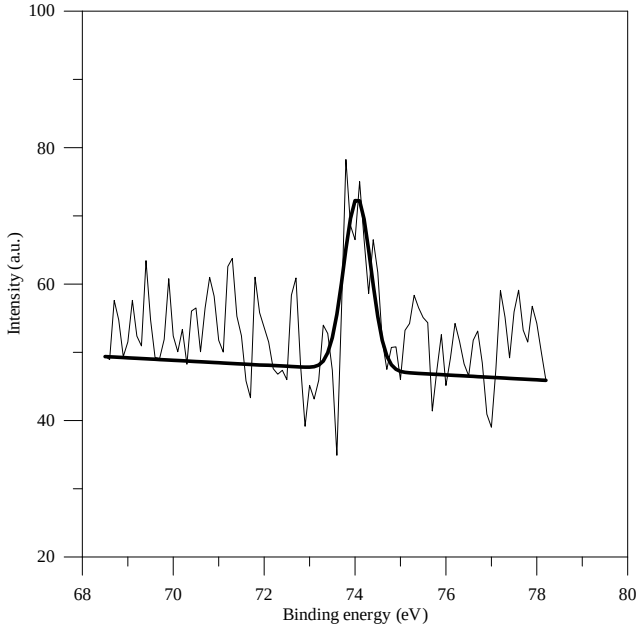

Fig. 5. Al2p photoelectron peak in the XPS spectrum of the 10% Al doped film

3.3 Electrical results

Hall Effect measurements were applied to characterize the electrical properties of the undoped ZnO and Al-doped ZnO thin films. Measurements were made at room temperature and carried out in a constant magnetic field of 0.54 T and with a current value set at 1 nA with HMS-3000. The ohmic contacts were made by soldering indium metal to the four corners of the square shaped sample. Several Hall parameters such as carrier concentration, mobility, resistivity, sheet concentration and conductivity for the films were obtained. To ensure reliability of the results, the Hall measurements were repeated several times for each sample the results of the Hall Effect measurements were summarized in Table 1.

Table 1. The results of the Hall Effect measurements

	Carrier concentration ($1/cm^3$)	Mobility ($cm^2/V\ s$)	Resistivity (ohm cm)	Conductivity (1/ohm cm)	Carrier type
Al 0%	3.803×10^{16}	31.8	5.153×10^{0}	1.941×10^{-1}	n
Al 2%	2.912×10^{17}	23.2	9.218×10^{-1}	1.085×10^{0}	n
Al 4%	5.050×10^{17}	35.9	3.436×10^{-1}	2.910×10^{0}	n
Al 6%	1.338×10^{18}	42.1	1.107×10^{-1}	9.030×10^{0}	n
Al 10%	2.495×10^{17}	43.7	5.287×10^{-1}	1.891×10^{0}	n

As seen in Table 1, the electrical properties of Al doped films were detected to affect by doping. With increase of doping levels from 0 to 10%, the conduction type was detected to not change. With the increase of doping levels from 0 to 6%, resistivity of the ZnO films was revealed to decrease from -5.153×10^{0} ohm cm to 1.107×10^{-1} ohm cm. The similar effect was seen in reference 29. The compared to the undoped ZnO with a carrier concentration of 3.803×10^{16} ($1/cm^3$), Al doped ZnO films were exhibited 10^{17} and 10^{18}. The resistivity variation of films with different doping concentrations was displayed in Fig. 6.

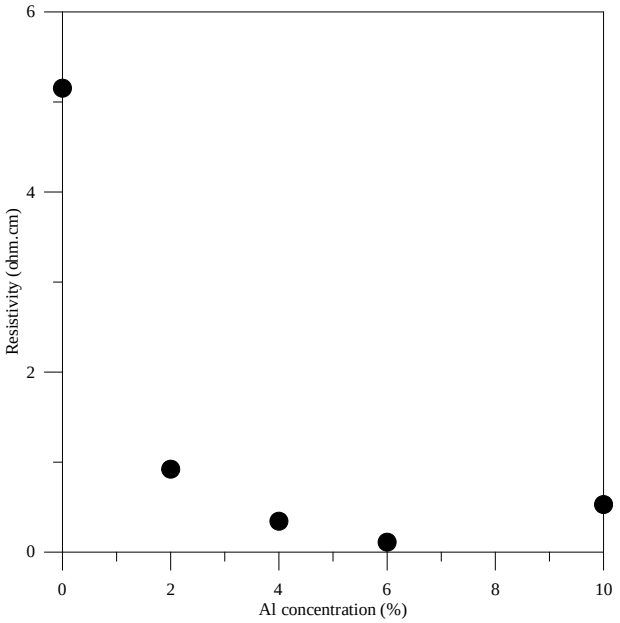

Fig. 6. The resistivity of ZnO films at various Al dopant concentrations

With the increase of doping levels from 0 to 6%, the carrier concentration of the ZnO films were believed to increase as a result of one extra donor electrons from the Al dopant, and associated oxygen vacancies [31,43-45]. So, Al^{3+} ions subsituted Zn^{2+} ions in the ZnO lattice. This alteration was detected to cause an increase in carrier concentration and a decrease in resistivitiy [33]. After reaching a minium value in 6% Al doped films minimum, the resistivity increased in 10% Al concentration. Increasing of the Al doped, was caused to reduce the carrier concentration. The excess Al atoms might be segregated into the grain boundaries at the doping concentration of 10 %.

3.4 Effect of doping concentration on photovoltaic effect

Photovoltaic effect is known to cause owing to the light activated electron generation at the depletion region of p-Si that is close to the heterojunction interface. It is also known that AZO film is highly permeable in the visible region (T > 90%) and this permits the visible light to pass through it [46]. The light is firstly absorbed under p-Si layer, for AZO/p-Si heterojunction. This is caused to produce electron-holes pairs. Under reverse bias conditions, this pairs generates the photocurrent. The high carrier concentration of AZO films constitutes a depletion region near to p-Si region and a potential structural barrier. Due to the electric field that generated in the depletion region, the photon-generated electrons diffuse towards the positive electrode on the AZO layer, while UV photons are initially absorbed in the AZO layer. As a result, this causes an increase in current with increasing reverse bias. On the other hand, the p-Si surface provides the source of electrons that can enter into the AZO films. The generated coupling current flows owing to the charge exchange between the valence-bands and the conduction of the silicon by recombination and production [46,47]. The films prepared as the doped and undoped, showed the rectifier characteristic in the dark. It is shown in Figs. 7,8,9,10,11 that all of the generated heterojunctions under the halogen light illumination, are clearly a photovoltaic effect.

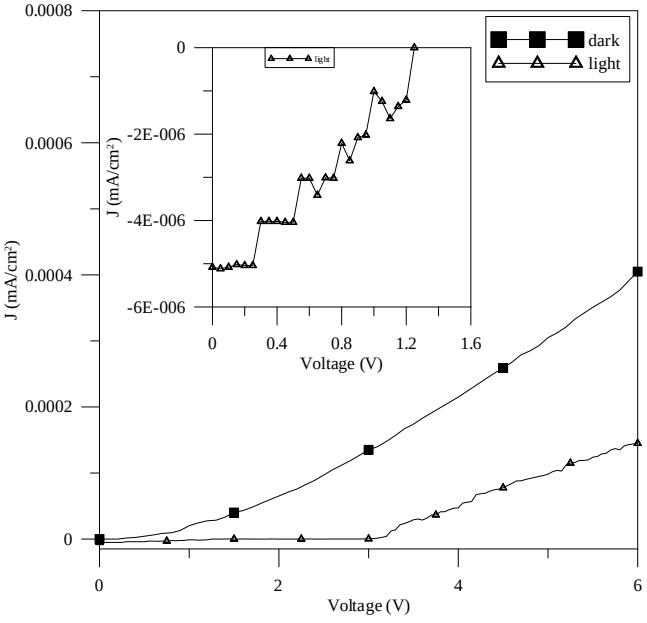

Fig. 7. Current density vs. voltage characteristics of undoped ZnO

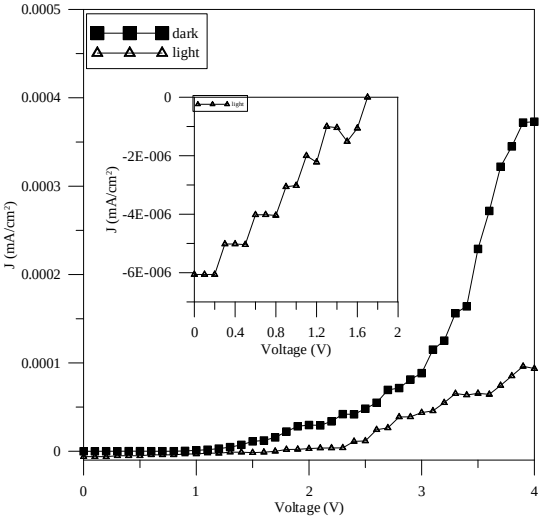

Fig. 8. Current density vs. voltage characteristics of the 2% Al doped film

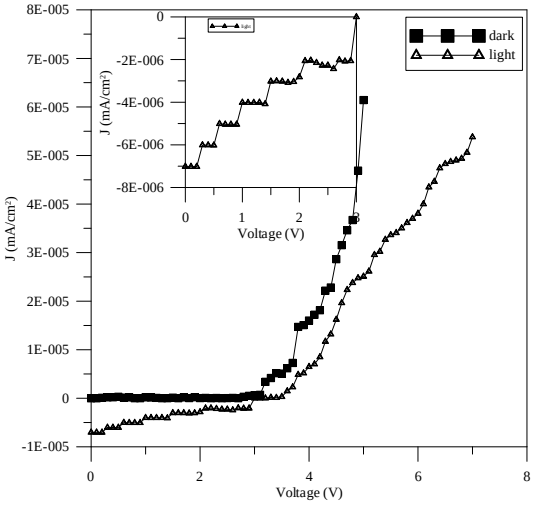

Fig. 9. Current density vs. voltage characteristics of the 4% Al doped film

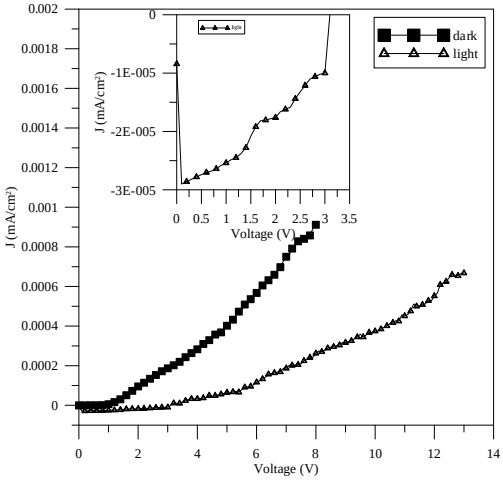

Fig. 10. Current density vs. voltage characteristics of the 6% Al doped film

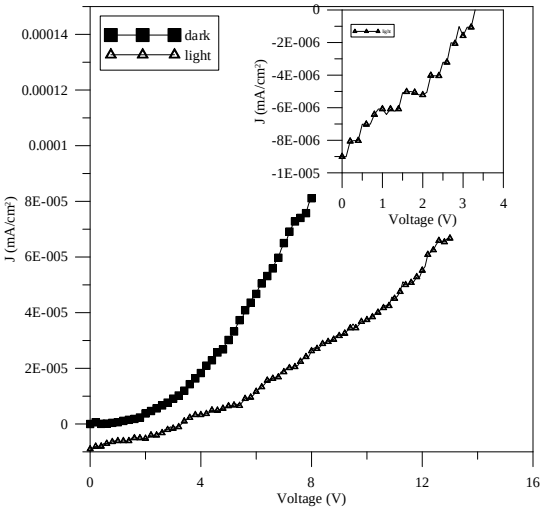

Fig. 11. Current density vs. voltage characteristics of the 10% Al doped film

When the Table 2 was examined, the open-circuit voltages and the short circuit currents of AZO/p-Si heterojunctions with the different Al concentration were observed.

Table 2. Open circuit voltage and short circuit current for heterojunctions with different Al doping concentrations in ZnO films

Al concentration(%)	V_{oc}(v)	I_{sc}(mA)x10^{-6}
0	1.25	5.08
2	1.7	6.06
4	3	7.01
6	3.1	8.43
10	3.3	9.00

It was determined to the increase in the open-circuit voltages and the short circuit currents with increasing Al concentrations. This photovoltaic effect indicated to the increasing by entered Al atoms into ZnO films. This increase could be connected the decrease in the resistances of films due to the Zn substitution of Al on the doping. When Al^{3+} displaces by Zn^{2+}, the additional free charge carriers were produced and consequently the transmission mechanism was increased. As seen in Hall measurements, the carrier concentration was increased by Al doping according to undoped films. Because of this, the structural potential in heterojunctions was detected to increase with the Al increasing. Accordingly, the open circuit voltage also increased. Also, the carriers under the high structural

potential effect caused the large short-circuit current [48,29].

4. Conclusions

Undoped ZnO and Al-doped ZnO thin films were grown by PFCVAD technique. The effects of doping with different Al concentrations on the electrical and photovoltaic properties of ZnO were examined. It was observed at one mode about 439 cm^{-1} of the undoped ZnO and Al-doped ZnO (AZO) thin films that were prepared different Al concentrations. Although Zn2p and Ols peaks were observed in undoped ZnO and doped ZnO with 2%, 4% and 6% concentration of Al, Al2p peaks were not encountered. Al2p peak was only seen in the doped ZnO film with 10% Al. With the increase of doping levels from 0 to 6%, resistivity of the ZnO films decreased. As seen in photovoltaic property, the prepared films by the doped and undoped, showed the rectifier characteristic in the dark. The open-circuit voltages and the short circuit currents of AZO/p-Si heterojunctions with the different Al concentration were observed. It was determined to the increase in the open-circuit voltages and the short circuit currents with increasing Al concentrations.

References

[1] A. Janotti, C. G. V. Walle, Rep. Prog. Phys., **72**, 126501 (2009).

[2] H. Yamada, Y. Ushimi, M. Takeuchi, Y. Yoshino, T. Makino, S. Arai, Vacuum, **74**, 689 (2004).

[3] K. Tominaga, T. Murayama, I. Mori, T. Okamoto, K. Hiruta, T. Moriga, I. Nakabayashi, Vacuum, **59**, 546 (2000).

[4] H. Qi, Q. Li, C. Wang, L. Zhang, L. Lv, Vacuum, **81**, 943 (2007).

[5] Z. Y. Xiao, Y. C. Liu, D. X. Zhao, J. Y. Zhang, Y. M. Lu, D. Z. Shen, X. W. Fan, Journal of Luminescence, **122–123**, 822 (2007).

[6] J. Y. Lee, Y. S. Choi, W. H. Choi, H. W. Yeom, Y. K. Yoon, J. H. Kim, S. Im, Thin Solid Films, **420 –421**, 112 (2002).

[7] K. D. Takci, E. Senadim Tuzemen, K. Kara, S. Yilmaz, R. Esen, O. Baglayan, J. Mater. Sci: Mater. Electron., **25**, 2078 (2014).

[8] A. Mahmood, N. Ahmed, Q. Raza, T. M. Khan, M. Mehmood, M. M. Hassan, N. Mahmood, Phys. Scr., **82**, 065801 (2010).

[9] C. Guillén, J. Herrero, Thin Solid Films, **480–481**, 129 (2005).

[10] M. Emziane, K. Durose, N. Romeo, A. Bosio, D. P. Halliday, Thin Solid Films, **480**, 377 (2005).

[11] F. H. Wang, H. P. Chang, C. C. Tseng, C. C. Huang, H. W. Liu, Current Applied Physics, **11**, S12 (2011).

[12] W. Yang, J. Joo, Current Applied Physics, **12**, S99 (2012).

[13] Y. Zhu, R. J. Mendelsberg, J. Zhu, J. Han, A. Anders, Applied Surface Science, **265**, 738 (2013).

[14] J. Gao, R. Chen, D. H. Li, L. Jiang, J. C. Ye, X. C. Ma, X. D. Chen, Q. H. Xiong, H. D. Sun, T. Wu, Nanotechnology, **22**, 195706 (2011).

[15] Q. H. Li, D. Zhu, W. Liu, Y. Liu, X. C. Ma, Applied Surface Science, **254**, 2922 (2008).

[16] D. Song, A. G. Aberle, J. Xia, Appl. Surf. Sci., **195**, 291 (2002).

[17] X. Jiang, F. L. Wong, M. K. Fung, S. T. Lee, Appl. Phys. Lett., **83**, 1875 (2003).

[18] H. Kim, J. S. Horwitz, G. P. Kushto, Z. H. Kafafi, D. B. Chrisey, Appl. Phys. Lett., **79**, 284 (2001).

[19] M. Vishwas, K. Narasimh Rao, A. R. Phani, K. V. Arjuna Gowda, R. P. S. Chakradhar, Solid State Communications, **152**, 324 (2012).

[20] H. W. Lee, S. P. Lau, Y. G. Wang, K. Y. Tse, H. H. Hng, B. K. Tay, Journal of Crystal Growth, **268**, 596 (2004).

[21] C. H. Ahn, H. Kim, H. K. Cho, Thin Solid Films, **519**, 747 (2010).

[22] C.-A. Tseng, J.-C. Lin, Y.-F. Chang, S.-D. Chyou, K.-C. Peng, Applied Surface Science, **258**, 5996 (2012).

[23] C. S. Prajapati, A. Kushwaha, P. P. Sahay, Materials Chemistry and Physics, **142**, 276 (2013).

[24] J. Li, J. Xu, Q. Xu, G. Fang, Journal of Alloys and Compounds, **542**, 151 (2012).

[25] H. Bo, M. Z. Quan, X. Jing, Z. Lei, Z. N. Sheng, L. Feng, S. Cheng, S. Ling, Z. C.Yue, Y. Z. Shan, Y. Y. Ting, Materials Science in Semiconductor Processing, **12**, 248 (2009).

[26] A. A. Al-Ghamdi, O. A. Al-Hartomy, M. E. Okr, A. M. Nawar, S. El-Gazzar, F. El-Tantawy, F. Yakuphanoglu, Spectrochimica Acta Part A: Molecular and Biomolecular Spectroscopy, **131**, 512 (2014).

[27] S. Sarkar, S. Patra, S. K. Bera, G. K. Paul, R. Ghosh, Physica E, **46**, 1 (2012).

[28] Y. Caglar, Müjdat Caglar, Saliha Ilican, Current Applied Physics, **12**, 963 (2012).

[29] W. Zhang, Z. Z. Liu, Y. Han, Z. Fu, Optoelectron. Adv. Mater. – Rapid Comm, **4**, 681 (2010).

[30] S. Venkatachalam, Y. Iida, Y. Kanno, Superlattices and Microstructures, **44**, 127 (2008).

[31] Y.-H. Tseng, J.-S. Wang, Thin Solid Films, **534**, 186 (2013).

[32] L. C. Gontijo, R. Machado, V. P. Nascimento, Materials Science and Engineering B, **177**, 780 (2012).

[33] P.-H. Lei, C.-M. Hsu, Y.-S. Fan, Organic Electronics, **14**, 236 (2013).

[34] Y. Zhang, G. Du, X. Yang, B. Zhao, Y. Ma, T. Yang, H. C. Ong, D. Liu, S. Yang, Semicond. Sci. Technol., **19**, 755 (2004).

[35] K. J. Chen, T. H. Fang, F. Y. Hung, L. W. Ji, S. J. Chang, S. J. Young, Y. J. Hsiao, Applied Surface Science, **254**, 5791 (2008).

[36] A. Khan, J. Pak. Mater. Soc., **4**, 5 (2010).

[37] L. Li, L. Fang, X. J. Zhou, Z. Y. Liu, L. Zhao, S. Jiang, Journal of Electron Spectroscopy and Related Phenomena, **173**, 7 (2009).

[38] M. Chen, X. Wang, Y. H. Yu, Z. L. Pei, X. D. Bai, C. Sun, R. F. Huang, L. S. Wen, Appl. Surf. Sci., **158**, 134 (2000).
[39] T. Prasada Rao, M. C. Santhosh Kumar, A. Safarulla, V. Ganesan, S. R. Barman, C. Sanjeeviraja, Phys. B, **405**, 2226 (2010).
[40] J. F. Moulder, W. F. Stickel, P. E. Sobol, K. D. Bomben, Handbook of X-ray Photoelectron Spectroscopy: A Reference Book of Standard Spectra for Identi_cation and Interpretation of XPS Data; Physical Electronics Division, Perkin-Elmer Corporation: Eden Prairie, MN, USA, (1995)
[41] K. Uma, M. Rusop, T. Soga, T. Jimbo, Jpn. J. Appl. Phys., **46**, 40 (2007).
[42] E. Senadim Tuzemen, H. Sahin K. Kara, S. Elagoz, R. Esen, Turkish Journal of Physics, **38**, 111 (2014).
[43] Hu. Jianhua, Roy G. Gordon, J. Appl. Phys., **71**, 880 (1992).
[44] K. E. Lee, M. Wang, E. J. Kim, S. H. Hahn, Curr. Appl. Phys., **9**, 683 (2009).
[45] R. K. Shukla, A. Srivastava, A. Srivastava, K. C. Dubey, Journal of Crystal Growth, **294**, 427 (2006).
[46] T. Holloway, R. Mundle, H. Dondapati, M. Bahoura, A. K. Pradhan, Chemical Physics Letters, **534**, 48 (2012).
[47] H. Bo, M. Z. Quan, X. Jing, Z. Lei, Z. N. Sheng, L. Feng, S. Cheng, S. Ling, Z. C.Yue, Y. Z. Shan, Y. Y. Ting, Materials Science in Semiconductor Processing, **12**, 248 (2009).
[48] T. Ganesh, S. Rajesh, Francis P. Xavier, Materials Science in Semiconductor Processing, **16**, 295 (2013).

*Corresponging author: esenadim@cumhuriyet.edu.tr